

Two- and three-particle Bose-Einstein correlations in small collision systems at LHCb

Miłosz Zdybał, Institute of Nuclear Physics PAS, Kraków, Poland

On behalf of the LHCb Collaboration

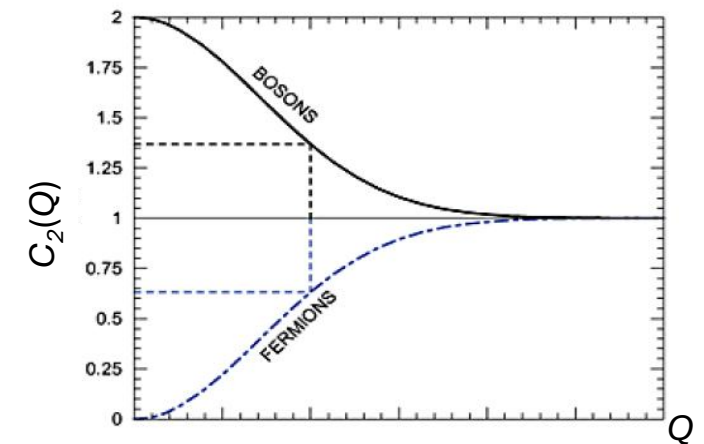


Quantum correlations in particle physics

- G. Goldhaber, S. Goldhaber, W. Lee and A. Pais, 1959
 - Bevalac/LBL experiment in Berkeley
 - Observation of the resonances by comparing Q distribution of unlike-sign pion pairs to same-sign – unexpected angular correlation [Phys. Rev. 120, 300]
- Correlations in four-momenta of indistinguishable particles emitted from the same source

$$Q_{12} = \sqrt{-(k_1 - k_2)^2} = \sqrt{M^2 - 4\mu^2}$$

- Total wave function:
 - Bosons: symmetrization– Bose-Einstein Correlations
 - Fermions: anti-symmetrization – Fermi-Dirac Correlations
- Useful tool to probe spatial and temporal structure of hadronization region



Two-pion correlation function

Definition

- $C_2(k_1, k_2) = \frac{P(k_1, k_2)}{P(k_1)P(k_2)}$

- Parametrisation:

- Levy parameterization with $\alpha_L = 1$ + long range correlations

$$C_2(Q) = N(1 + \lambda_2 e^{-(RQ)^{\alpha_L}}) \times (1 + \delta \cdot Q)$$

Experimentally

- $C_2(Q) = \frac{N(Q)^{DATA}}{N(Q)^{REF}}$

- Reference sample: event mix – different events, the same VELO multiplicity

R – the radius of a spherical static source

λ_2 – the intercept parameter (correlation strength)

N – normalization factor

δ – long-range correlations

Double ratio

- Improved correlation function
$$r_d(Q) = \frac{C_2^{\text{data}}(Q)}{C_2^{\text{sim}}(Q)}$$
- Reduce possible imperfections in the construction of the reference sample,
- Eliminate second order effects to large extent,
- Correct for long range correlations (if properly simulated)
- Construction of the double ratio should mitigate:
 - single particle acceptance and efficiency,
 - effects due to the detector occupancy, acceptance and material,
 - selection cuts,
 - two-track efficiency effects if properly simulated.

Three-pion correlation function and parameterization

Coulomb corrections factorized according to
Generalised Riverside Method [Phys. Rev. C 92, 014902]

$$G_3(Q_{12}, Q_{13}, Q_{23}) \approx G_2(Q_{12})G_2(Q_{13})G_2(Q_{23})$$

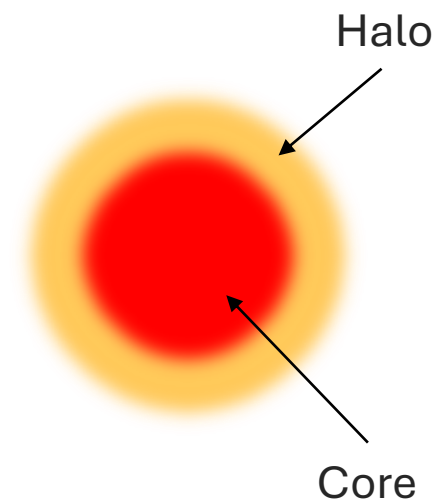
$$C_3(Q_{12}, Q_{13}, Q_{23}) = N(1 + \delta_{12}Q_{12})(1 + \delta_{13}Q_{13})(1 + \delta_{23}Q_{23})G_3(Q_{12}, Q_{13}, Q_{23})C_3^{(0)}(Q_{12}, Q_{13}, Q_{23})$$

$$C_3^{(0)}(Q_{12}, Q_{13}, Q_{23}) = C_2^{(0)}(Q_{12})C_2^{(0)}(Q_{13})C_2^{(0)}(Q_{23}) = \frac{1}{1 + \ell_3 e^{-0.5(|Q_{12}R|^{\alpha_L} + |Q_{13}R|^{\alpha_L} + |Q_{23}R|^{\alpha_L})} + \ell_2(e^{-|Q_{12}R|^{\alpha_L}} + e^{-|Q_{13}R|^{\alpha_L}} + e^{-|Q_{23}R|^{\alpha_L}})}$$

- Levy-type $C_3^{(0)}$ function of the Q_{12}, Q_{13}, Q_{23} of the pion triplet
- $C_3(Q_{12}, Q_{13}, Q_{23})$ can be expressed as a convolution of $C_2(Q_{12}), C_2(Q_{13}), C_2(Q_{23})$

Core-halo model

- Results of analysis interpreted within the framework of the core-halo model [Z. Phys. C71, 491 (1996), Eur. Phys. J. C (1999) 9, 275] as it is done in the Phenix experiment [T. Novak, arXiv:1801.03544]
- Core
 - Direct production of pions
 - Hydrodynamic evolution or particle production from excited strings, followed by subsequent re-scattering of the particles
- Halo
 - Core is surrounded by pions emitted from the decay of long-lived hadronic resonances (ω , η , η' , K^0) which are treated as belonging to the hadronic source



Core-halo model parameters

- Fraction of the core f_c
 - Partially coherent emission p_c
- } Can be used to express two- and three-body correlation strengths

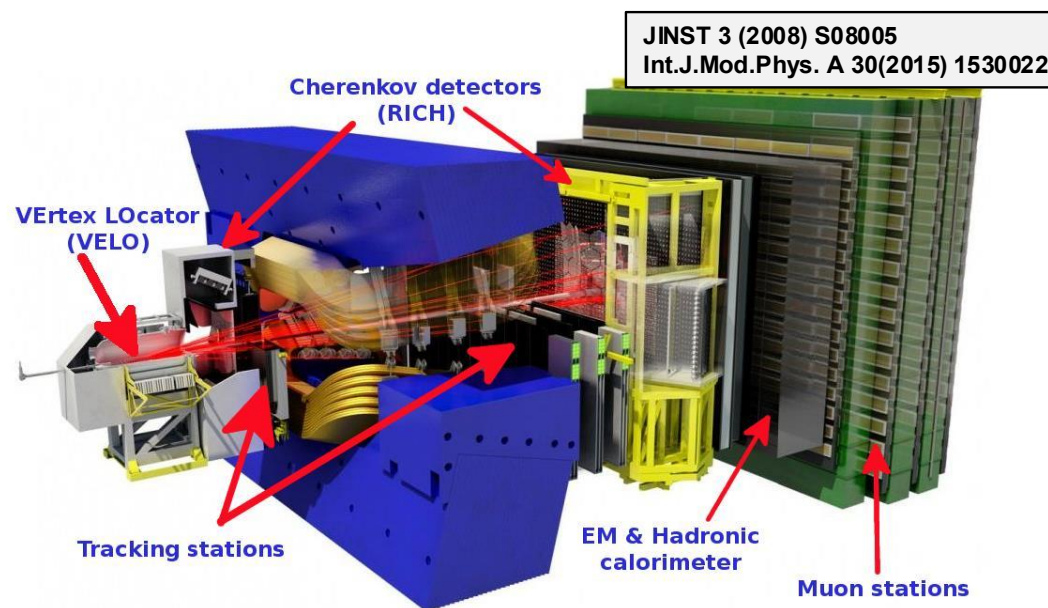
$$f_c^2[(1 - p_c)^2 + 2p_c(1 - p_c)] = \lambda_2$$

$$2f_c^3[(1 - p_c)^3 + 3p_c(1 - p_c)^2] + 3f_c^2[(1 - p_c)^2 + 2p_c(1 - p_c)] = \lambda_3$$

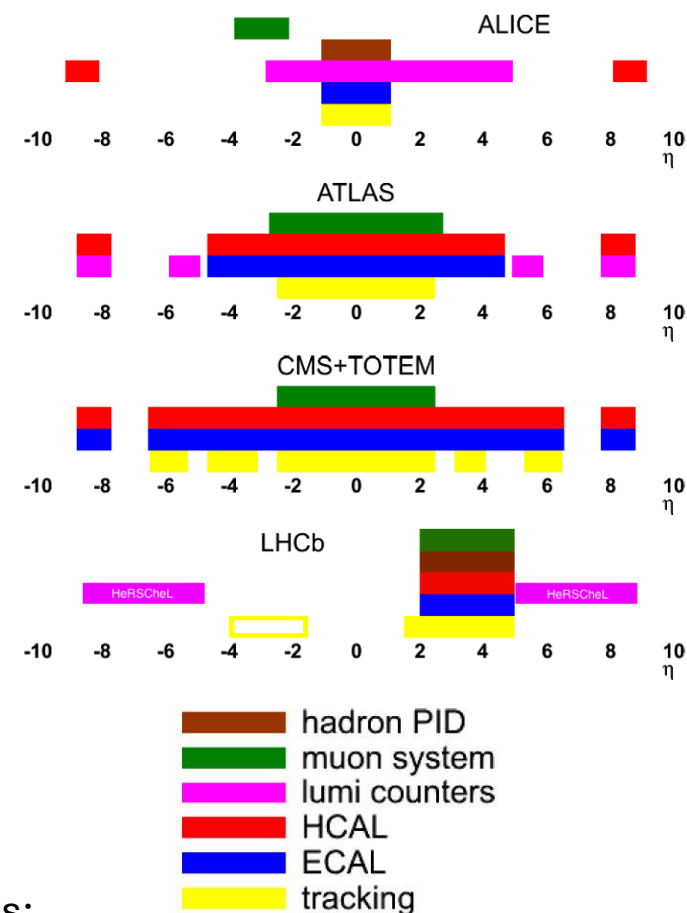
- Correlation strength $\lambda_3 = \ell_3 + 3\ell_2$ (ℓ_3, ℓ_2 are the fit parameters)
- κ_3 – function of the correlation strengths, can indicate presence additional effects in the core

$$\kappa_3 = 0.5(\lambda_3 - 3\lambda_2)/\lambda_2^{3/2}$$

The LHCb experiment



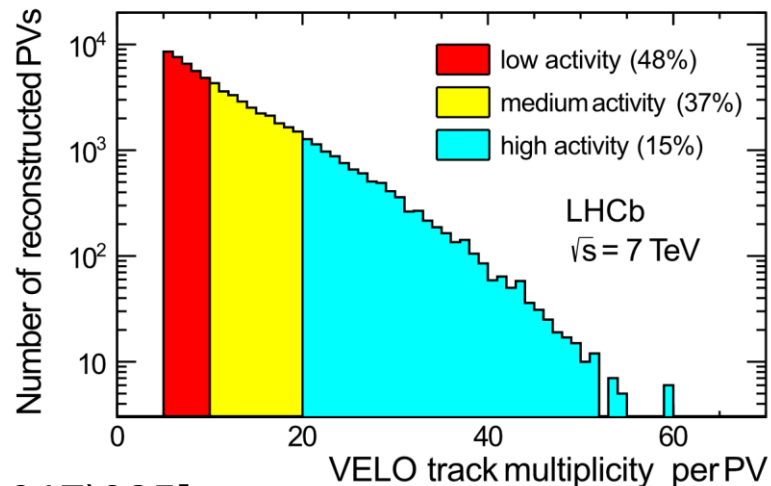
- Acceptance: $2 < \eta < 5$
- Impact parameter resolution: $20 \mu\text{m}$
- Momentum resolution: $\Delta p/p = 0.5 - 1.0\%$ (5-200 GeV/c)
- Fully instrumented in the forward region
- Detector designed for flavour physics and searches for physics beyond SM, but also provides:
 - Complementary results to the other LHC experiments



Data samples

Proton-proton

- Collected in 2011 at a centre-of-mass energy $\sqrt{s} = 7$ TeV,
- Integrated luminosity of 1.0 fb^{-1} ,
- Divided into 3 bins of VELO-track multiplicity.

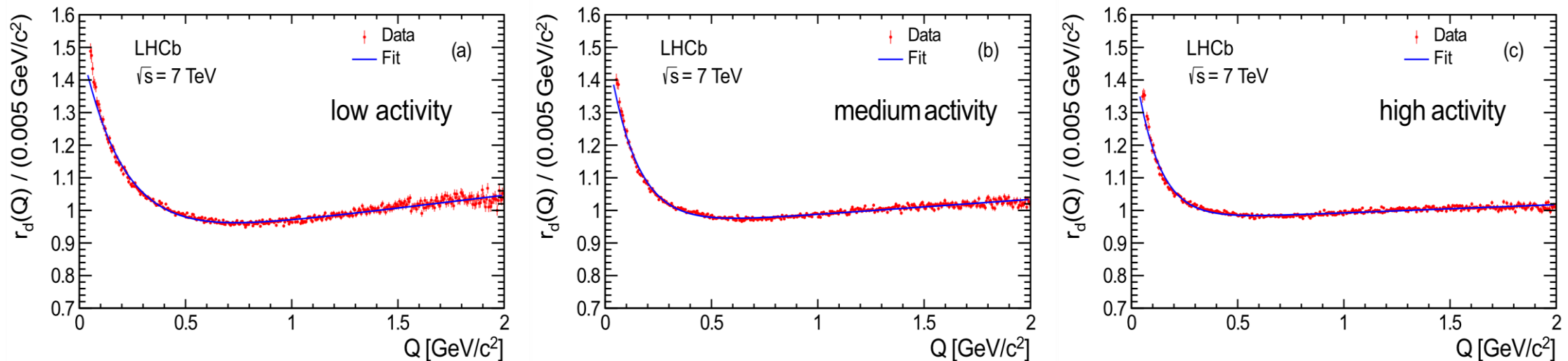


Proton-lead, lead-proton

- Collected in 2013 at a nucleon-nucleon centre-of-mass energy $\sqrt{s_{NN}} = 5.02$ TeV,
- Two collision modes: $p\text{Pb}$ and $\text{Pb}p$,
- Integrated luminosities of 1.06 nb^{-1} ($p\text{Pb}$) and 0.52 nb^{-1} ($\text{Pb}p$)
- Divided into 18 bins of VELO-track multiplicity.

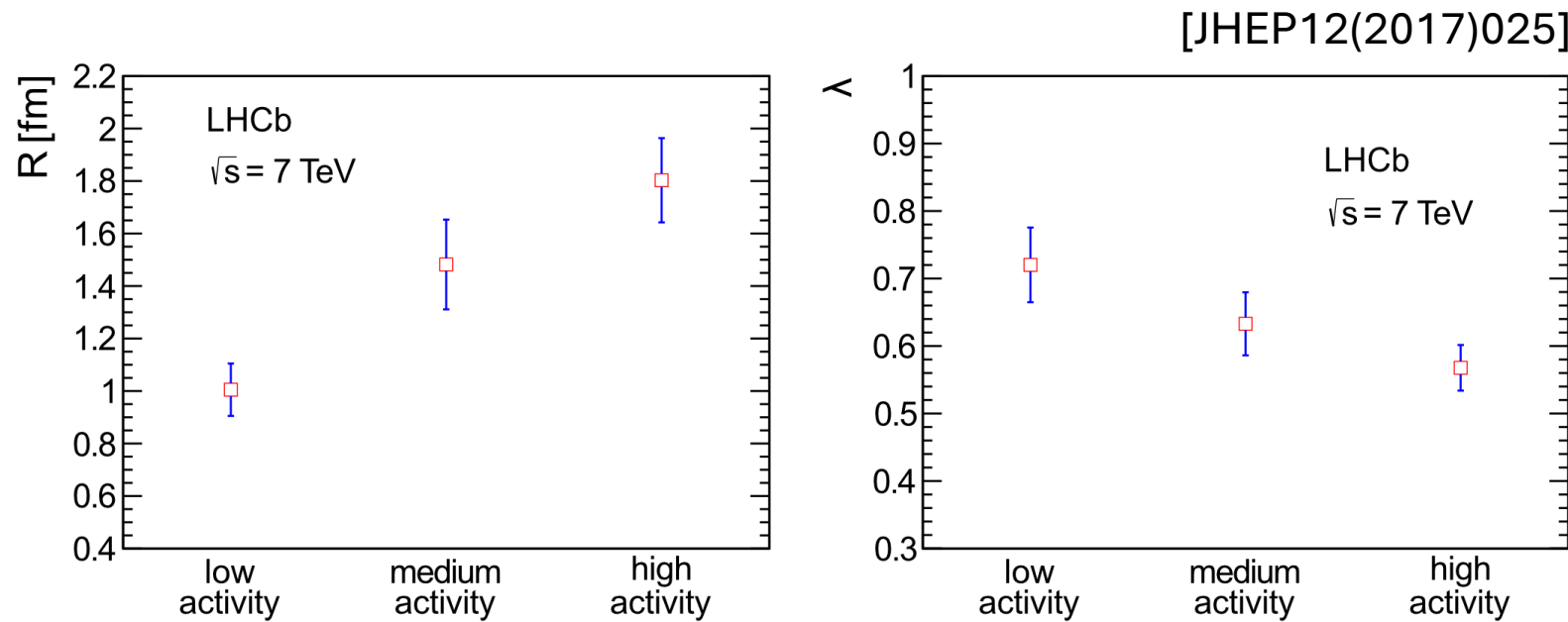
Two-pion Bose-Einstein correlations in proton-proton collisions

[JHEP12(2017)025]



- Fitted correlation function in different bins of activity (number of reconstructed tracks of charged particles in the VELO detector),
- Bose-Einstein correlations visible as an increase in signal for low Q values

Two-pion Bose-Einstein correlations in proton-proton collisions

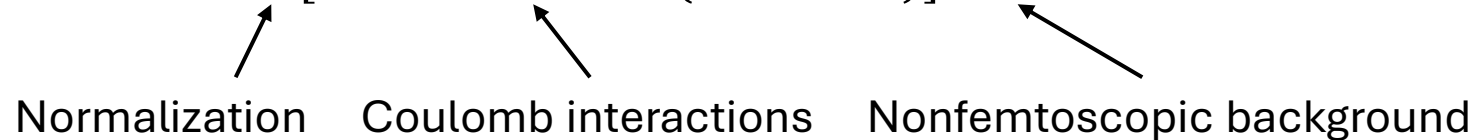


- Dependence of the fit parameters on the activity class,
- Confirms observations by LEP and other LHC experiments.

Correlation function for proton-lead

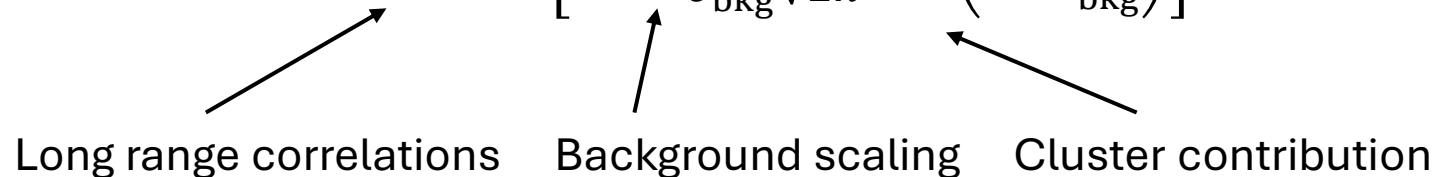
- Correlation function parameterization including electromagnetic effects and the nonfemtoscopic background, using Bowler-Sinyukov formalism with Levy parameterization with $\alpha_L = 1$ for BEC signal:

$$C_2(Q) = N[1 - \lambda + \lambda K(Q) \times (1 + e^{-|RQ|})] \times \Omega(Q)$$


 Normalization Coulomb interactions Nonfemtoscopic background

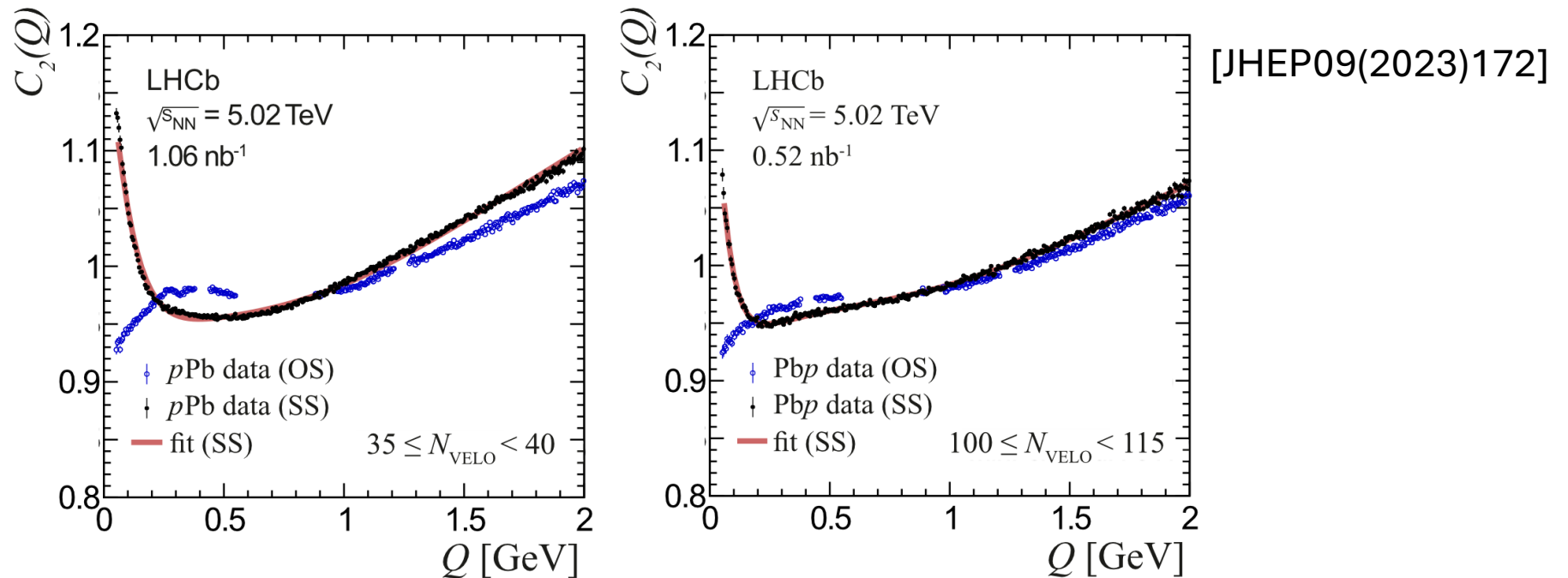
- Correlation function for opposite sign pions used to investigate nonfemtoscopic background contribution:

$$\Omega(Q) = (1 + \delta Q) \times \left[1 + z \frac{A_{\text{bkg}}}{\sigma_{\text{bkg}} \sqrt{2\pi}} \exp\left(-\frac{Q^2}{2\sigma_{\text{bkg}}^2}\right) \right]$$


 Long range correlations Background scaling Cluster contribution

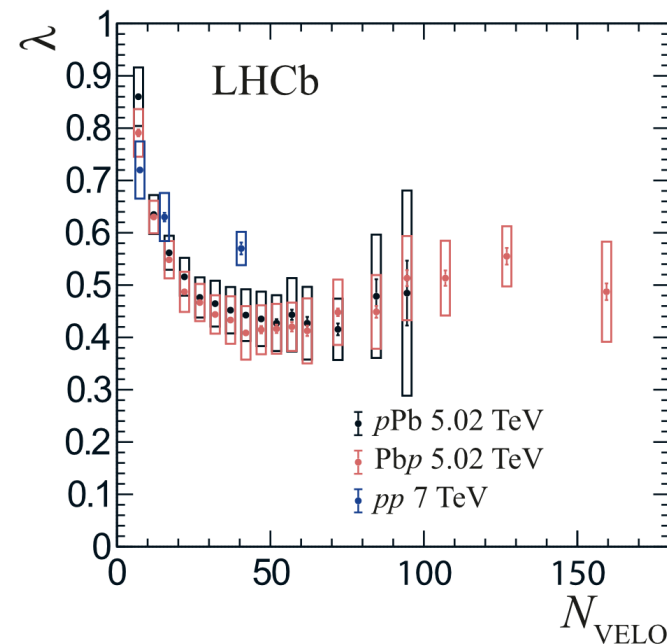
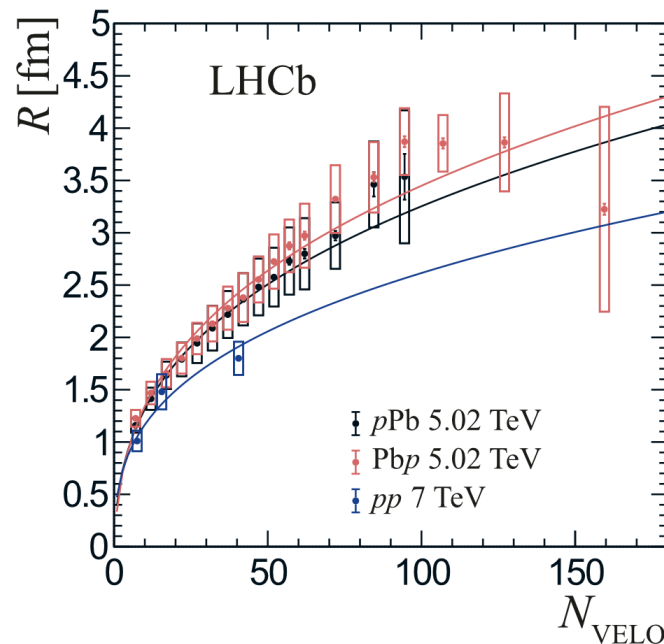
Full parameterization
in JHEP09(2023)172

Two-pion Bose-Einstein correlations in proton-lead and lead-proton collisions



- Fitted correlation function for same sign pions (black) – calculate the correlation parameters,
- Correlation function for opposite sign pions (blue, no BEC) – estimate the cluster contribution in each bin.

Two-pion Bose-Einstein correlations in proton-lead, lead-proton and proton-proton collisions

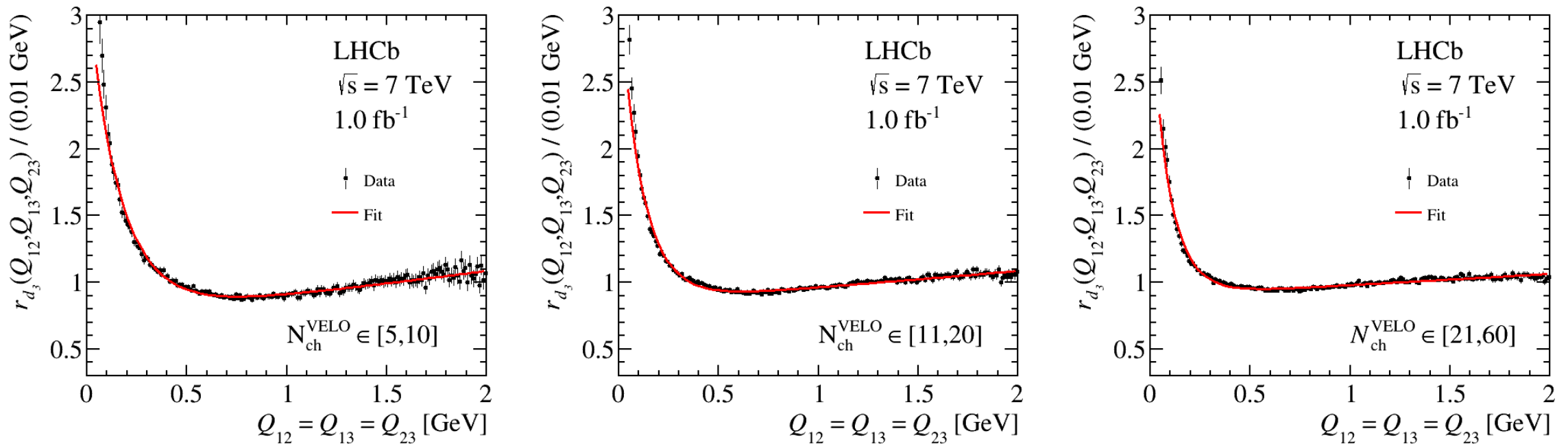


[JHEP09(2023)172]

- Measured correlation radii scale with the cube root of the charged particle multiplicity – compatible with predictions based on hydrodynamic models,
- Differences related to the beam direction – hint for a potential sensitivity to the rapidity.

Three-pion Bose-Einstein correlations in proton-proton collisions

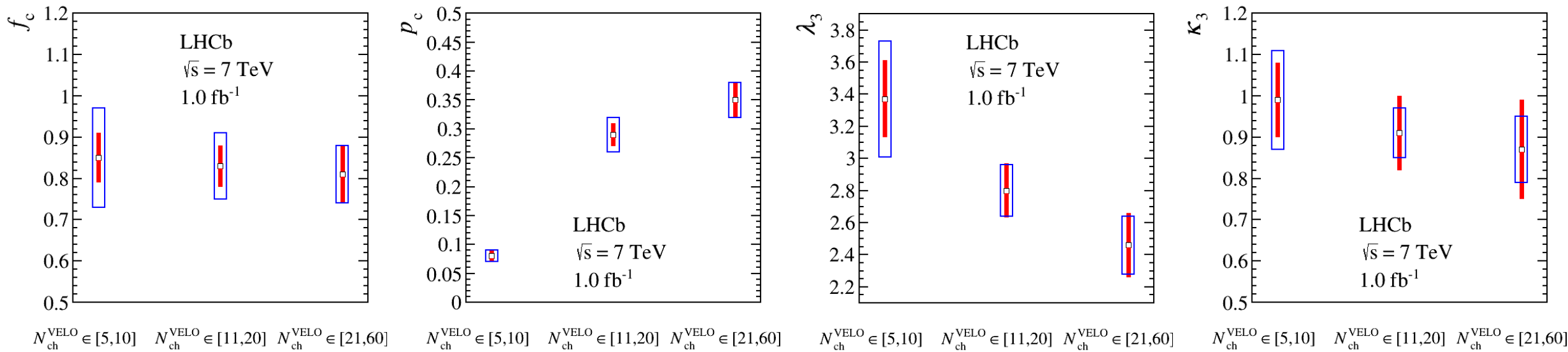
[LHCb-PAPER-2025-007, arXiv:2506.03072]



- Correlation functions fitted in different bins of charged particles multiplicity,
- Fit uses values of R and λ_2 from the two-body analysis.

Three-pion Bose-Einstein correlations in proton-proton collisions

[LHCb-PAPER-2025-007, arXiv:2506.03072]



- Partial coherence seen in p_c increases significantly with charged particle multiplicity,
- Central values of κ_3 under unity, but within uncertainties.

Conclusions

- Correlation radii and intercept parameters (correlation strengths) measured for pp and pPb collisions:
 - R scales with the cube root of the charged particle multiplicity – compatible with predictions based on hydrodynamic models,
 - For pp , R and λ_2 slightly lower than measured by ATLAS for corresponding interaction multiplicities,
 - Sensitivity of the correlation parameters to the rapidity hinted by comparison different directions of the pPb beam
- Three-body correlations interpreted in the core-halo model:
 - Fraction of the pions emitted from the core not dependent on the charged particle multiplicity,
 - Measured parameters suggest partially coherent emission of pions.

Backup slides

Binning of $p\text{Pb}$ and $\text{Pb}p$ samples

bin#	N_{VELO}	Sample fraction [%]	
		$p\text{Pb}$	$\text{Pb}p$
1	5–9	< 2	< 2
2	10–14	2	2
3	15–19	4	2
4	20–24	7	3
5	25–29	10	4
6	30–34	13	5
7	35–39	14	6
8	40–44	10	5
9	45–49	10	6
10	50–54	8	6
11	55–59	7	7
12	60–64	5	6
13	65–79	6	15
14	80–89	—	7
15	90–99	—	7
16	100–114	—	6
17	115–139	—	7
18	140–179	—	4

Systematic uncertainties for three-body BEC

$$N_{\text{ch}}^{\text{VELO}} \in [5,10]$$

Source	σ_{λ_3} [%]	σ_{f_c} [%]	σ_{p_c} [%]	σ_{κ_3} [%]
Event generator	8.7	10.4	9.7	10.4
PV multiplicity	5.9	8.6	8.3	4.7
PV reconstruction	< 1.0	0.1	0.1	< 0.1
Fit binning	0.7	0.1	0.4	1.2
Fit low-Q range	0.3	0.6	1.0	0.3
Fit high-Q range	0.4	0.5	0.5	0.3
Fake tracks	2.1	2.4	2.4	1.8
$P(\pi)$	2.1	2.7	1.8	3.3
Total	11.0	14.0	13.2	12.1

$$N_{\text{ch}}^{\text{VELO}} \in [11,20]$$

Source	σ_{λ_3} [%]	σ_{f_c} [%]	σ_{p_c} [%]	σ_{κ_3} [%]
Event generator	3.6	5.1	5.0	3.2
PV multiplicity	2.1	5.0	5.0	2.1
PV reconstruction	1.1	1.6	1.6	1.1
Fit binning	1.1	1.1	1.1	1.1
Fit low-Q range	1.4	1.5	1.8	2.5
Fit high-Q range	1.8	1.9	1.8	2.1
Fake tracks	1.8	4.3	4.3	1.8
$P(\pi)$	2.1	1.7	1.4	3.9
Total	5.7	9.0	9.0	6.8

$$N_{\text{ch}}^{\text{VELO}} \in [21,60]$$

Source	σ_{λ_3} [%]	σ_{f_c} [%]	σ_{p_c} [%]	σ_{κ_3} [%]
Event generator	2.4	2.8	2.8	0.4
PV multiplicity	3.3	5.3	5.4	3.7
PV reconstruction	2.4	2.5	2.4	2.8
Fit binning	1.0	0.4	0.7	2.0
Fit low-Q range	1.8	2.4	3.0	3.7
Fit high-Q range	3.0	3.4	3.4	3.3
Fake tracks	2.0	2.1	2.2	2.4
$P(\pi)$	4.1	3.9	3.7	5.7
Total	7.5	8.9	9.1	9.4